Advanced Physical Research
Vol.5, No.3, 2023, pp.156-167

# INFLUENCE OF EXTERNAL ELECTRIC FIELD AND STRAIN ON THE SPIN STATE OF NiXY MONOLAYER (X/Y = Cl, Br, I)

**Tran Tung-Bach[1], Nguyen Vo Phuong-Binh[1], Hoang Ngoc Cam-Tu[1], Hoang Trong-Phuc[2,3,*], Pham Duc-Thinh[4], Doan Phan Thao-Tien[4], Tran Tuan-Anh[1*]**

[1]Ho Chi Minh City University of Technology and Education, Ho Chi Minh, Vietnam
[2]Laboratory Center, Duy Tan University, Da Nang, Vietnam
[3]Institute of Research and Development, Duy Tan University, Danang, Vietnam
[4]Nhatrang Institute of Technology Research and Application, Vietnam Academy of Science and Technology, Nha Trang, Vietnam

**Abstract.** Our study demonstrates the possibility of two distinct methods to manipulate the quantum state, specifically the spin state of a NiXY monolayer (X/Y=Cl, Br, I). In the first case, application of an external electric field along the c-axis of the monolayer results in a spin that aligns with the electric field direction. For NiICl, NiClBr, and NiBrI monolayers, with the upper layer having heavier halide elements and the lower layer consisting of lighter halide elements, the spin state reverses when a c-axis electric field is applied in the opposite direction. The energy difference between the spin-up and spin-down states increases with increasing electric field magnitude, resulting in a corresponding increase in the probability of Ni atom spin reversal. The second approach to controlling the spin state of a NiXY monolayer involves stretching or contracting its material layer. Our modeling results reveal that for both NiICl and NiBrI monolayers, the ground spin state of the material can change with the application of strain, but such an effect is not observed in NiClBr.

***Keywords:*** *2D material, external electric field, strain, density functional theory, spin state.*

***Corresponding Authors:*** *Hoang Trong-Phuc, Laboratory Center and Institute of Research and Development, Duy Tan University, Danang, Vietnam, email: hoangtrongphuc@dtu.edu.vn*
*Tran Tuan-Anh, Faculty of Applied Sciences, Ho Chi Minh City University of Technology and Education, Ho Chi Minh City, Vietnam, e-mail: anhtt@hcmute.edu.vn*

***Received:*** *15 June 2023;* ***Accepted:*** *26 July 2023;* ***Published:*** *03 October 2023.*

## 1. Introduction

In recent years, two-dimensional (2D) magnetic materials have gained substantial traction and show great potential in various applications. Transition metal atoms are commonly found in these materials, and they arrange in a planar hexagonal lattice reminiscent of graphene. Due to their unique structures and two-dimensional nature, 2D magnetic materials are of great interest, particularly their strong magnetic abilities that emerge from the unpaired electrons of transition metal atoms. Their inherent high conductivity and broad range of electrical and optical properties also make them a choice material for the development of electronics, optoelectronics, spintronic, and magnetic

**How to cite (APA):**
Tran, T.B., Nguyen, V.P.B., Hoang, N.C.T., Hoang, T.P., Pham, D.T., Doan, P.T.T., & Tran, T.A. (2023). Influence of external electric field and strain on the spin state of NiXY monolayer (X/Y = Cl, Br, I). *Advanced Physical Research, 5*(3), 156-167.

memory. Current standard electronic devices operate by electron movement in semiconductors like silicon, but with Moore's law (Pollie, 2021) effect, reducing device size, especially those dependent on silicon, is challenging. Employing spin-electron processes in spin-electron transport-based devices, which are appropriate for low-power consumption applications, offers one solution. Therefore, identifying the fundamental ferromagnetism in 2D van der Waals (vdW) crystals is crucial for comprehending and investigating the magnetism origin that promotes spin transmission (Ehsan *et al.*, 2022). Recently, vdW layered transition metal compounds have been recognized as viable prospects for developing 2D ferromagnetic (FM) semiconductors, as exfoliating them off of their inherent magnetism results in monolayers. Several metal-based two-dimensional (2D) material systems, such as $VSe_2$, $MnSe_2$, $FePS_3$, $MnO_2$, and $Fe_3GeTe_2$, have been identified as intrinsic ferromagnetic (FM) metals, albeit with low Curie temperatures below room temperature (Cong *et al.*, 2019). It is worth noting that these materials do not display semiconductor FM (Torun *et al.*, 2015; Zhuang *et al*., 2015; Wang *et al*., 2016). Therefore, to produce magnetism in 2D semiconductor materials, techniques such as doping, defect engineering, and adatom adsorption have been studied (Kulish et al., 2015; Krasheninnikov *et al*., 2009; Wang *et al*., 2015; Gobbi *et al.*, 2020).

In a recent study, (Mounet *et al.*, 2018) utilized high-throughput computational methods to examine 5619 known layered compounds and identified thirteen readily exfoliable 2D ferromagnetic semiconductors, including monolayers of $NiI_2$, $NiBr_2$, and CrOCl. Theoretical analysis suggests that the $NiI_2$ monolayer may have a higher $T_C$ (>70K) than the $CrI_3$ monolayer and the $Cr_2Ge_2Te_6$ bilayer (Kulish & Huang, 2017; Lu *et al*., 2019). Additionally, a new class of 2D materials, called Janus 2D materials, has drawn significant interest as of late. These materials possess chemically asymmetric top and bottom surfaces, with distinct halide anions occupying the top layer sites and being sandwiched between a layer of metal atoms in the monolayer Janus, breaking its symmetry. These materials present intriguing characteristics including integrated polarization, piezoelectricity, and catalysis, among others. The Janus NiXY monolayer family (X, Y = Cl, Br, I, $X \neq Y$) can be easily constructed from $NiX_2$ monolayers. Recent findings reveal that this family of Janus NiXY monolayers is stable and possesses out-of-plane piezoelectricity (Guo *et al*., 2022).

Nevertheless, no research has been conducted yet to investigate the electrical and magnetic characteristics of these materials under the impact of electric fields and strain. Thus, it is paramount to investigate families of monolayer semiconductor materials with ferromagnetic characteristics to clarify the intrinsic mechanism of ferromagnetic semiconductors. In spin-dependent data processing applications, it is important to understand how to manipulate magnetization or spin by applying electrical effects to the antimagnetic material under consideration (Ehsan *et al*., 2022). $NiX_2$ has been reported to possess robust ferromagnetic features that make it appropriate as a magnetic layer in information retrieval and storage systems to ensure reliability among various 2D van der Waals (vdW) ferromagnets. In this study, we theoretically predicted the family of magnetic monolayer halides NiXY (X=Cl, Br, and I), which exhibit remarkable stability. Using density functional theory (DFT) calculations, we analyzed how external electric fields and strain affect the electricity and magnetization properties of monolayer NiXY.

## 2. Method calculation

All of the computations are performed utilizing the density functional theory (DFT) in the QUANTUM ESPRESSO software package (Giannozzi *et al*., 2009), in parallel with the PAW (projector augmented wave) method (Blöchl, 1994) to process core electrons. The generalized gradient approximation (GGA) was utilized to determine exchange and correlation energies, with the Perdew – Burke – Ernzerhof (PBEsol) gradient-corrected functional being used. PBEsol is a PBE correction method created principally for solid-state calculations. PBEsol has been demonstrated to be accurate for solids under intense compression, in contrast to real solids and their surfaces, where exchange takes precedence over correlation, having truly slowly varying correlations (Perdew *et al.*, 2008). Furthermore, to estimate strong electronic correlations and handle the strong in-situ Coulomb interaction of local electrons whose positions are not precisely specified by the GGA functional, the Hubbard theory (U) (Dudarev *et al*., 1998) is employed, as proposed by (Liechtenstein *et al*., 1995). A U value typically ranging from 1 eV to 7 eV is suggested to adjust the band gap appropriately for the experiment. A vacuum space of 20 Å is employed equidistant from either side of the membrane to prevent contact between nearby layers when calculating the monolayer NiX2 material (X=Cl, Br, I) and the precise Janus NiXY monolayer structure (X, Y = Cl, Br, I, $X \neq Y$). Brillouin zone integration was done using the Monkhorst-Pack meshing method with a special k-points grid of $8 \times 8 \times 1$. Wavefunctions on the wave plane were studied in the energy range with an 80 Ry threshold. The atomic positions and lattice constants of the monolayers were relaxed using the Broyden-Fletcher-Goldfarb-Shanno (BFGS) (Perdew, Burke, & Ernzerhof, 1996) quasi-Newton algorithm with a convergence threshold of the force acting on each atom $10^{-5}$ Ry/bohr and for the total energy $10^{-6}$ Ry.

## 3. Results and discussion

### *3.1. Monolayer $NiX_2$*

In this study, we present the findings on the electromagnetic characteristics of $NiX_2$ and NiXY monolayers. In addition, we aimed to explore the influence of external factors on the magnetic attributes of these materials, which result in modifications of the monolayer structure. As a first step, we conducted a structural examination of $NiX_2$, where X denotes Cl, Br, or I. The monolayers of $NiX_2$ feature a structure that is analogous to 1T-$MoS_2$ monolayers. In this arrangement, the Ni transition metal is situated in the central position, and it is surrounded by two layers of halogen atoms. Each Ni atom forms octahedral geometry, coordinating with six halogen ligands. We provide a table that contains the parameters characterizing the structure of $NiX_2$, which were estimated using computational methods (Table 1). The outcomes of our analyses suggest an increasing trend in lattice constants and $d_{Ni-X}$, $d_{X-X}$ bonds as atomic radii increase, moving from Cl to I. Our results regarding lattice constants are in good agreement with prior research carried out on bulk structures, both experimentally and computationally (Kulish & Huang, 2017; McGuire, 2017).

Having obtained earlier findings (Kulish & Huang, 2017; Lu *et al*., 2019) indicating that the ground magnetic state of $NiX_2$ monolayers is ferromagnetic (FM), we proceeded to carry out energy band structure calculations using the GGA+U method with $U$ = 4eV for the $NiX_2$ monolayers in their FM state. Figure 1 showcases the respective energy band structures and PDOS of the $NiX_2$ monolayers. Our results demonstrate that all three

materials are indirect semiconductors and have corresponding bandgaps of 1.9503 eV, 1.34 eV, and 0.6371 eV for $NiCl_2$, $NiBr_2$, and $NiI_2$, respectively. We postulate that the decrease in the band gap from $NiCl_2$ to $NiI_2$ can be linked to the weakening of the crystal field, which is inversely proportional to the Ni-X bond length. An analysis of Partial Density of States (PDOS) reveals that the states contributing to the highest valence band (VBM) and the lowest conduction band (CBM) mostly comprise Ni-d and halogen-p hybrid orbitals. These findings corroborate earlier calculations (Lu *et al*., 2019).

**Table 1.** Optimal structural parameters of $NiX_2$ (X = Cl, Br, I), including lattice constants a (Kulish & Huang, 2017), $a_{Exp}$ (McGuire, 2017), and $a_{DFT}$ (our calculation), $d_{Ni-X}$ bonds, $d_{X-X}$ distances between two halide planes, and bond angle (Ni-X-Ni).

| Compound | a (Å) | $a_{Exp}$ (Å) | $a_{DFT}$ (Å) | $d_{Ni-X}$(Å) | $d_{X-X}$ (Å) | Ni-X-Ni |
|---|---|---|---|---|---|---|
| $NiCl_2$ | 3.4434 | 3.48 | 3.48 | 2.3813 | 3.2900 | 92.608 |
| $NiBr_2$ | 3.6308 | 3.70 | 3.7 | 2.5252 | 3.5106 | 91.930 |
| $NiI_2$ | 3.8930 | 3.89 | 3.9 | 2.7088 | 3.7676 | 91.879 |

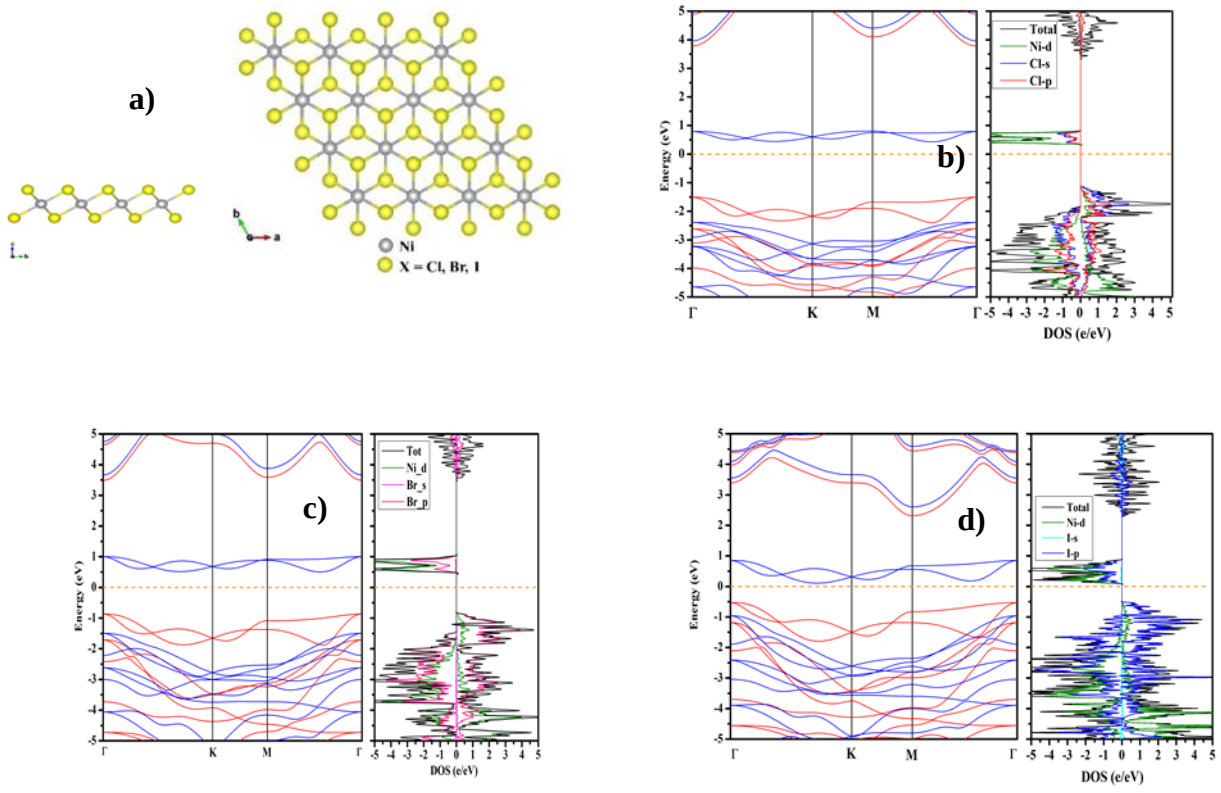


**Fig. 1.** (a) Top and side view of the optimized structure of $NiX_2$ (X = Cl, Br, I) and band structure and PDOS of (b) $NiCl_2$, (c) $NiBr_2$, and (d) $NiI_2$ monolayers

### *3.2. Monolayer NiXY*

After obtaining the optimal structures for the $NiX_2$ monolayers, we constructed the structures of Janus NiXY monolayers by replacing one of the atomic layers of Cl/Br/I from $NiCl_2$/$NiBr_2$/$NiI_2$ with an atomic layer of Br/I/Cl, respectively. The Janus compounds adopt a sandwich-like crystal structure, as depicted in Figure 2, with the Ni layer sandwiched between two layers of halide anions while being coordinated by ligands in an octahedral field strain, where three atoms of the upper halide anion layer and three atoms of the lower halide anion layer comprise the coordination sphere. This crystal structure breaks the symmetry, leading to some fascinating effects that we will elaborate on in the next section. In Figure 2, the state corresponds to the spin-up configuration, with the Ni spin directed along the c-axis of the lattice. Conversely, in the spin-down state, the Ni spin is rotated in the opposite direction. We present the optimal structural parameters, including lattice constant *a*, bond length $d_{Ni-X}$, $d_{Ni-Y}$, $d_{X-Y}$, and bond angle Ni-X-Ni and Ni-Y-Ni, in Table 2. The lattice constant values of NiXY decrease with the sum of the ionic radii X and Y, and for each NiXY monolayer, $d_{Ni-X}$ is larger than $d_{Ni-Y}$. These findings are in agreement with the calculations of (Gorkan *et al*., 2023).

**Table 2.** The optimal structural parameters of NiXY (X/Y = Cl, Br, I), such as the lattice constant *a* (Gorkan *et al*., 2023) and $a_{DFT}$ (our calculation), bond length $d_{Ni-X}$ from Ni to heavier halide ion and $d_{Ni-Y}$ from Ni to the lighter halide ion, the distance between the two halides planes $d_{X-Y}$, bond angle (Ni-X-Ni) and (Ni-Y-Ni).

| **Compound** | **a (Å)** | **$a_{DFT}$ (Å)** | **$d_{Ni-X}$(Å)** | **$d_{Ni-Y}$(Å)** | **$d_{X-Y}$ (Å)** | **Ni-X-Ni (º)** | **Ni-Y-Ni (º)** |
|---|---|---|---|---|---|---|---|
| NiClBr | 3.5403 | 3.59 | 2.5085 | 2.4029 | 3.4006 | 89.766 | 94.896 |
| NiBrI | 3.7728 | 3.84 | 2.5638 | 2.6816 | 3.6400 | 89.400 | 94.748 |
| NiICl | 3.696 | 3.75 | 2.6730 | 2.4499 | 3.5305 | 87.490 | 97.948 |

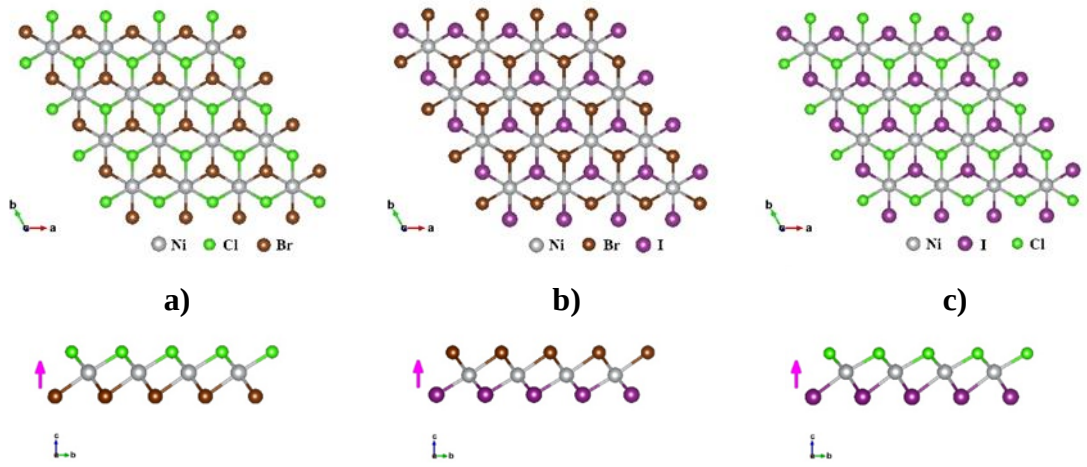


**Fig. 2.** Top and side view of the optimized structure of a) NiClBr, b) NiBrI and c) NiICl

Subsequently, we examined the energy band structure of FM state for NiXY monolayers using GGA+U method with U = 4. Figure 3 illustrates the energy band structure and PDOS of these monolayers. The obtained outcomes revealed that all three NiXY species are indirect semiconductors, with band gap widths of 1.4809, 0.6932, and 0.4716 eV for NiClBr, NiBrI, and NiICl, respectively. These values are notably lower than the band gaps of the $NiX_2$ monolayers. Analogous to the $NiX_2$ monolayers, the states in the vicinity of the valence band maximum and conduction band minimum regions of the NiXY monolayers are mainly contributed by the Ni-d and halogen-p hybridized orbitals.

### *3.3. Monolayer NiXY applied external electric field*

In various spintronic applications, quantum control (Ehsan *et al*., 2022), particularly spin manipulation via external electrical effects, is of paramount significance. For monolayer NiXY materials, their magnetic configuration is ferromagnetic (FM) (Guo *et al*., 2022), indicating that the spin-up state is the dominant state. However, the top and bottom Janus structure of these materials is asymmetrical, raising the possibility that the spin-down state could be the ground state of the material. Therefore, it is compelling to investigate the impact of external factors on the magnetic ground state (either spin-up or spin-down), which corresponds to the lowest energy state. Furthermore, we examine the influence of external factors on the energy band structure.

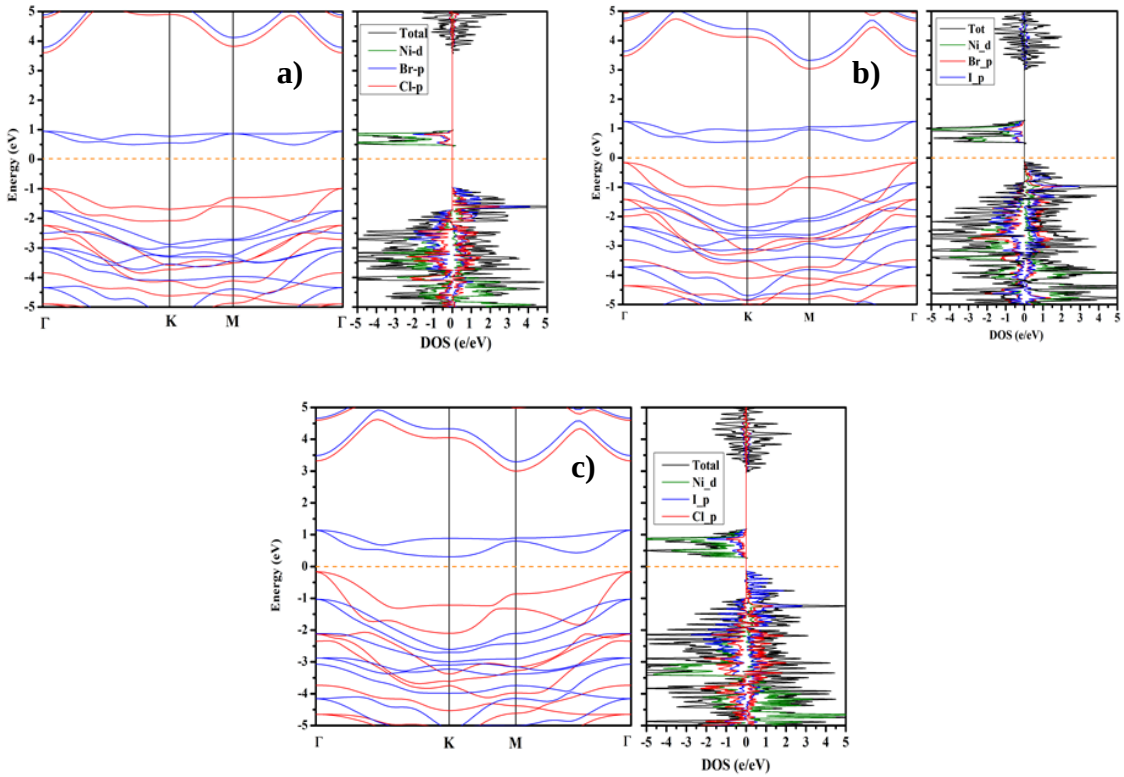


**Fig. 3.** Band structure and corresponding density of states of (a) NiClBr, (b) NiBrI, and (c) NiICl monolayers

Initially, to assess the external factors influencing the material, we investigate the impact of electric field on the spin state of NiXY. Following the optimization of monolayer structures of the NiXY materials, we summarize the calculated energy values for spin-up and spin-down states with input electric field values ranging from -4 to 4

V/nm as $\Delta E = E_{spin\text{-}up} - E_{spin\text{-}down}$ in Table 3. Moreover, Figure 4 depicts the dependence graph of ΔE as a function of electric field values for NiXY monolayers. It is evident that all three substances exhibit a similar trend: with electric field values < 0, negative ΔE values imply that the ground state corresponds to a spin-up state, while for electric field values > 0, positive ΔE values indicate that the ground state corresponds to a spin-down state. Notably, NiICl exhibits a larger slope in the graph, indicating that it is highly susceptible to changes in the electric field, followed by NiBrI and then NiClBr, which is the least sensitive. These findings suggest that electric field values affect the energies of the states and consequently, the spin for all three monolayers, i.e., NiClBr, NiBrI, and NiICl.

**Table 3.** Summary of $\Delta E = E_{spin\text{-}up} - E_{spin\text{-}down}$ values at varying external electric field for NiXY monolayers

| **NiICl** | | **NiBrI** | | **NiClBr** | |
|---|---|---|---|---|---|
| **Electric Field (V/nm)** | **ΔE (meV)** | **Electric Field (V/nm)** | **ΔE (meV)** | **Electric Field (V/nm)** | **ΔE (meV)** |
| -4 | -59.919 | -4 | -37.392 | -4 | -22.500 |
| -3 | -45.026 | -3 | -28.053 | -3 | -16.900 |
| -2 | -30.061 | -2 | -18.708 | -2 | -11.300 |
| -1 | -14.993 | -1 | -9.355 | -1 | -5.640 |
| 0 | -0.002 | 0 | -0.0008 | 0 | -1.010 |
| 1 | 14.989 | 1 | 9.355 | 1 | 5.630 |
| 2 | 30.054 | 2 | 18.706 | 2 | 11.200 |
| 3 | 44.949 | 3 | 28.053 | 3 | 17.500 |
| 4 | 59.840 | 4 | 37.389 | 4 | 22.500 |

The effects of external electric field on the energy band structures of NiXY monolayers were explored. Figure 5 depicts the energy band structures and PDOS at the ground magnetic state for NiClBr, NiBrI, and NiICl applied external electric field with values ranging from -4 to 4 V/nm. For NiClBr, the results obtained at -4; 0 and 4 V/nm external electric field were indicative of an indirect semiconductor, with the VBM point at Γ and the CBM point ranging between M and Γ. The associated band gap values for NiClBr were found to be 1.4482, 1.4679, and 1.4613 eV, respectively. Similarly, NiBrI exhibited results indicative of an indirect semiconductor, with the top of the CBM located to the left of K for electric field values of -4; 0 and 4 V/nm, with corresponding band gap values of 0.6535, 0.6932, and 0.6511 eV. Likewise, for NiICl, the results at all three electric field values (-4; 0 and 4 V/nm) were indicative of an indirect semiconductor from Γ → K with band gap values of 0.4616, 0.4777, and 0.4603 eV, respectively. Overall, the

electric field had a discernible but insignificant impact on the band gap value of NiXY monolayers. Examining the partial density of states (PDOS) of all three monolayers (NiClBr, NiBrI, and NiICl) at the three electric field values revealed that the regions near VBM are mainly contributed by halogen-p orbitals, while the regions near CBM are mainly contributed by hybridized Ni-d and halogen-p orbitals.

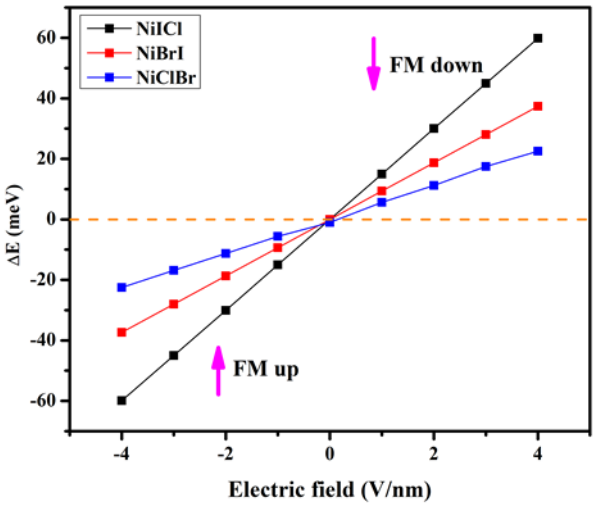


**Figure 4.** $\Delta E = E_{spin\text{-}up} - E_{spin\text{-}down}$ values at varying external electric field for NiXY monolayers

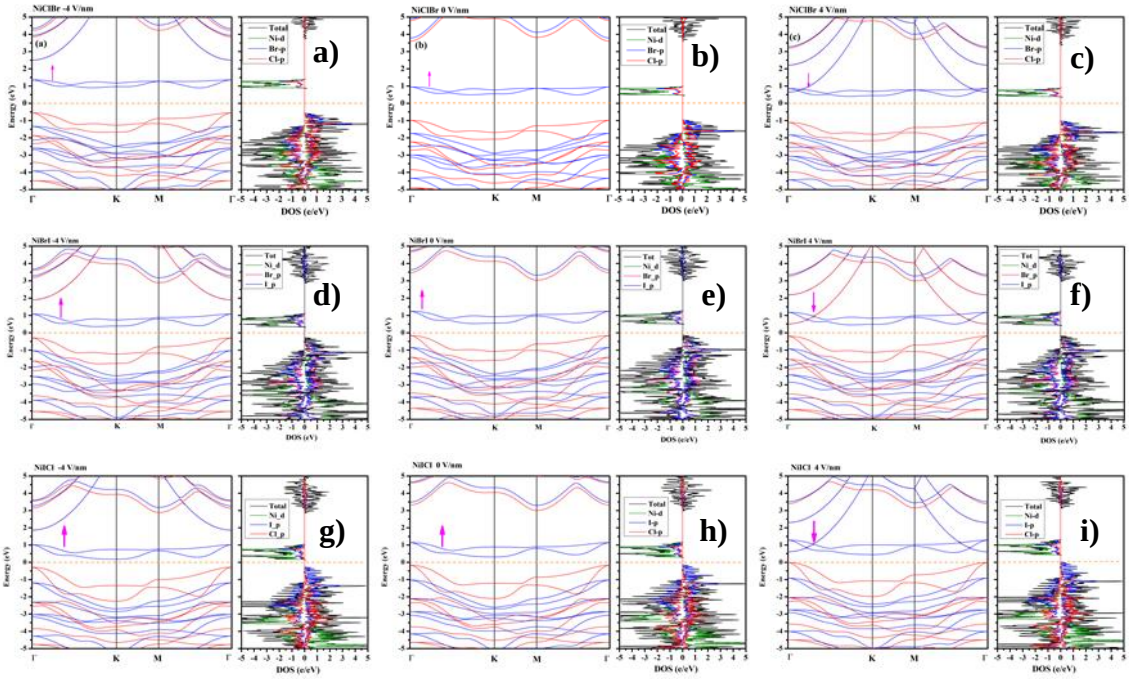


**Figure 5.** Band structure and PDOS of (a-c) NiClBr, (d-f) NiBrI, and (g-i) NiICl monolayers with the electric field from left to right is: -4, 0, 4 V/nm

### *3.4. Monolayer NiXY applied strain*

The impact of strain on the spin state of NiXY was investigated in this study. Table 4 presents the energy values acquired for the spin-up and spin-down structural states of NiXY with strain values ranging from -4% to 4% along the x-axis, calculated using the

equation $\Delta E = E_{spin\text{-}up} - E_{spin\text{-}down}$. Figure 6 illustrates the dependence of ΔE on the strain values of the NiXY monolayers. Our findings demonstrated that both NiICl and NiBrI followed the same trend: negative ΔE values corresponded to a spin-up state for the magnetic ground state under compressive strain values, while positive ΔE values revealed a spin-down state for the magnetic ground state under tensile strain values. Furthermore, NiICl exhibited a steeper slope than NiBrI, indicating greater susceptibility to changes in strain. Conversely, for NiClBr, ΔE values remained unchanged for all strain values. These results suggest that while strain can alter the spin of NiICl and NiBrI, it does not affect the spin of NiClBr.

**Table 4.** Variation of ΔE with Strain in NiXY Monolayers

| NiICl | | NiBrI | | NiClBr | |
|---|---|---|---|---|---|
| **Strain** | **ΔE meV** | **Strain** | **ΔE meV** | **Strain** | **ΔE meV** |
| -0.04 | -0.241 | -0.04 | -0.053 | -0.04 | -0.151 |
| -0.01 | -0.058 | -0.01 | -0.013 | -0.01 | -0.146 |
| 0 | -0.001 | 0 | -0.0008 | 0 | -0.150 |
| 0.01 | 0.051 | 0.01 | 0.010 | 0.01 | -0.138 |
| 0.04 | 0.192 | 0.04 | 0.042 | 0.04 | -0.134 |

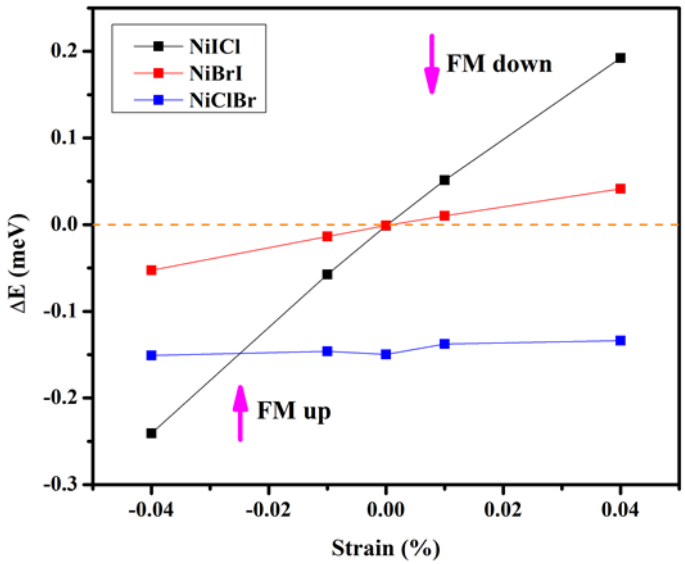


**Figure 6.** The Strain-Dependence of ΔE in NiXY monolayers

Figure 7 displays the Energy Band Structure and PDOS in the magnetic ground state for NiClBr, NiBrI, and NiICl for strain values ranging from -4 to 4%. The band

structure diagram for all three compounds exhibits clear spin separation, wherein the valence maximum (VBM) is contributed by spin-up, while the minimum conduction band is contributed by spin-down electrons. For NiClBr, the results reveal that it is an indirect semiconductor for all three strain values (-4%, 0%, and 4%). The VBM is at Γ, and the conduction band minimum (CBM) lies between M and Γ. The values of the band gap for NiClBr at -4%, 0%, and 4% strain values are 1.48099 eV, 1.4809 eV, and 1.49410 eV, respectively. For NiBrI, the results indicate that it is a semiconductor for all three deformation values (-4%, 0%, and 4%). The VBM peak is at Γ, and the left CBM peak is near point K. The values of the band gap for NiBrI at -4%; 0% and 4% deformation values are 0.356 eV, 0.694 eV and 0.7459 eV, respectively. Similarly, the computed band gap values of NiICl for all three cases (-4%, 0%, and 4%) show it to be an indirect semiconductor with distinct behavior for compressive strain value at -4% that skews the CBM point to the right of point K, while the VBM point is at Γ. In contrast, the VBM and CBM remain at Γ and K, respectively, for 0% and 4% tensile strain values. The values of the band gap for NiICl at -4%, 0%, and 4% strain values are 0.1466 eV, 0.4714 eV, and 0.5374 eV, respectively. Overall, it can be observed that the band gaps of NiBrI and NiICl show a significant decrease under the influence of compressive strain value at -4%, while NiClBr shows insignificant changes in band gaps. Conversely, with tensile strain at 4%, the band gap of all three substances increases. In addition, the observations from PDOS indicate that the states are sparser at strain values, but the regions surrounding the VBM and CBM are still mainly contributed by Ni-d and halogen hybrid orbitals -p.

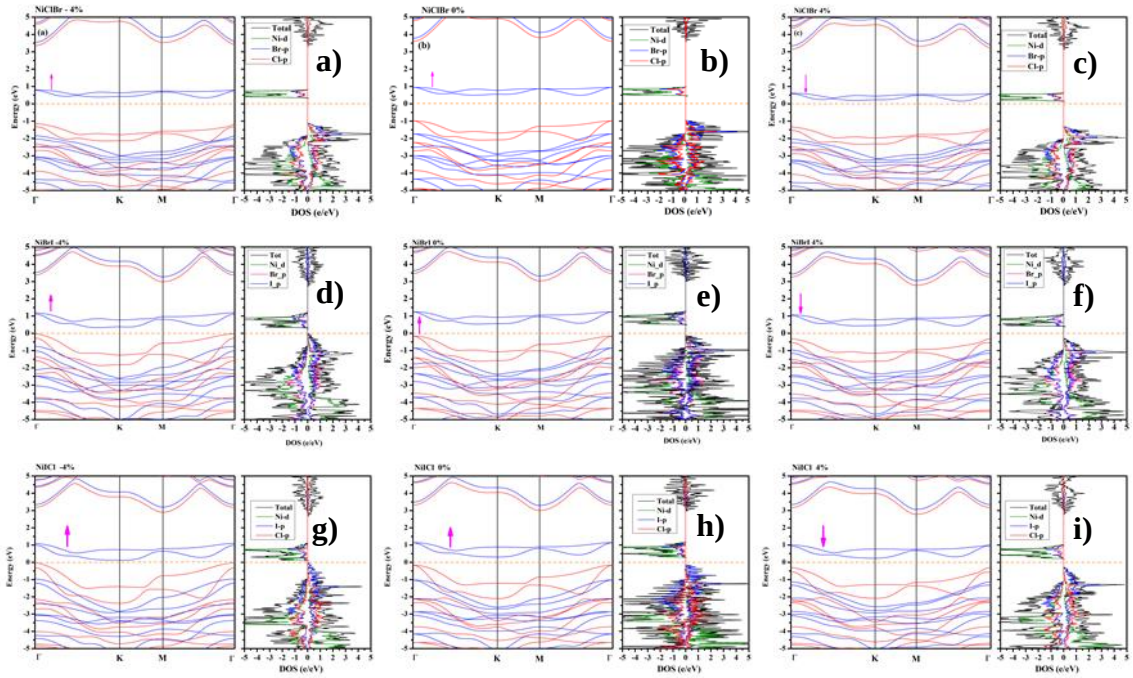


**Figure 7.** Band structure and corresponding density of states of (a-c) NiClBr, (d-f) NiBrI, and (g-i) NiICl monolayers with the strain from left to right is: -4, 0, 4 %

## 4. Conclusions

Our findings have successfully demonstrated two novel methods to manipulate the quantum state, particularly the spin state of a NiXY monolayer (X/Y=Cl, Br, I). In the first

approach, the application of an external electric field in the direction of the c-axis produces a spin that aligns with the electric field direction. We observed that for NiICl, NiClBr, and NiBrI monolayers, with the upper layer being composed of heavier halide elements and the lower layer being comprised of lighter halide elements, the spin state undergoes reversal when a c-axis electric field is applied in the opposite direction. Our results suggest that the energy gap between the spin-up and spin-down states increases with a rise in the magnitude of the electric field, leading to an upward trend in the probability of Ni atom spin reversal. The second method for controlling the spin state of a NiXY monolayer is based on stretching or contracting its material layer. Our computational analysis confirmed that the ground spin state of the material can be modified via the application of strain in both NiICl and NiBrI monolayers, although such an effect is not observed in NiClBr.

**Acknowledgment**

We thank the Ho Chi Minh City University of Technology and Education for providing financial support for us to complete this project – Code: SV2023-37.

**References**

Blöchl, P. (1994). Projector augmented-wave method. *Physical review B*, *50*(24), 17953.

Cong , W., Xieyu, Z., Linwei, Z., Ning-Hua, T., Zhong-Yi, L., & Wei, J. (2019). A family of high-temperature ferromagnetic monolayers with locked spin-dichroism-mobility anisotropy: MnNX and CrCX (X = Cl, Br, I; C = S, Se, Te). *Science Bulletin*, *64*(5), 293-300.

Dudarev, S., Botton, G., Savrasov, S., Humphreys, C., & Sutton, A. (1998). Electron-energy-loss spectra and the structural stability of nickel oxide: An LSDA+ U study. *Physical Review B*, *57*(3), 1505.

Ehsan , E., Ghulam , D., Ghazanfar, N., Sobia, N., Mudasar, B., Haroon, A. Q., & Muhammad, I. (2022). A review on two-dimensional (2D) magnetic materials and their potential applications in spintronics and spin-caloritronic. *Computational Materials Science*, 213, 111670.

Giannozzi, P., Baroni, S., Bonini, N., Calandra, M., Car, R., Cavazzoni, C., & Dabo, I. (2009). QUANTUM ESPRESSO: a modular and open-source software project for quantum simulations of materials. *Journal of physics: Condensed matter*, *21*(39), 395502.

Gobbi, S., Reinke, G., Gobbi, V., Rocha, Y., Sousa, T., & Coutinho, M. (2020). Biomaterial: concepts and basics properties. *Eur. Int. J. Sci. Technol.*, *9*(2), 23-42.

Gorkan, T., Das, J., Kapeghian, J., Akram, M., Barth, J., Tongay, S., Botana, A. (2023). Skyrmion formation in Ni-based Janus dihalide monolayers: Interplay between magnetic frustration and Dzyaloshinskii-Moriya interaction. *Physical Review Materials*, *7*(5), 054006.

Guo, S.-D., Zhu, Y.-T., Qin, K., & Ang, Y.-S. (2022). Large out-of-plane piezoelectric response in ferromagnetic monolayer NiClI. *Applied Physics Letters*, *120*(23), 232403.

Krasheninnikov, A., Lehtinen, P., Foster, A., Pyykkö, P., & Nieminen, R. (2009). Embedding transition-metal atoms in graphene: structure, bonding, and magnetism. *Physical Review Letters*, *102*(12), 126807.

Kulish, V. V., Huang, W. (2017). Single-layer metal halides MX2 (X= Cl, Br, I): Stability and tunable magnetism from first principles and Monte Carlo simulations. *Journal of Materials Chemistry C*, *5*(34), 8734-8741.

Kulish, V., Malyi, O., Persson, C., & Wu, P. (2015). Adsorption of metal adatoms on single-layer phosphorene. *Physical Chemistry Chemical Physics*, *17*(2), 992-1000.

Liechtenstein, A., Anisimov, V., & Zaanen, J. (1995). Density-functional theory and strong interactions: Orbital ordering in Mott-Hubbard insulators. *Physical Review B*, *52*(8), R5467.

Lu, M., Yao, Q., Xiao, C., Huang, C., & Kan, E. (2019). Mechanical, electronic, and magnetic properties of NiX2 (X= Cl, Br, I) layers. *ACS omega*, *4*(3), 5714--5721.

McGuire, M. (2017). Crystal and Magnetic Structures in Layered, Transition Metal Dihalides and Trihalides. *Crystals*, *7*(5), 121.

Mounet, N., Gibertini, M., Schwaller, P., Campi, D., Merkys, A., Marrazzo, A., & Pizzi, G. (2018). Two-dimensional materials from high-throughput computational exfoliation of experimentally known compounds. *Nature nanotechnology*, *13*(3), 246-252.

Perdew, J., Burke, K., & Ernzerhof, M. (1996). Generalized gradient approximation made simple. *Physical review letters*, *77*(18), 3865.

Perdew, J., Ruzsinszky, A., Csonka, G., Vydrov, O., Scuseria, G., Constantin, L., Burke, K. (2008). Restoring the density-gradient expansion for exchange in solids and surfaces. *Physical review letters*, *100*(13), 136406.

Pollie, R. (2021). *Nanosheet Chips Poised to Rescue Moore's Law*. Engineering.

Torun, E., Sahin, H., Bacaksiz, C., Senger, R., & Peeters, F. (2015). Tuning the magnetic anisotropy in single-layer crystal structures. *Physical Review B*, *92*(10), 104407.

Wang, H., Zhang, J., Hang, X., Zhang, X., Xie, J., Pan, B., & Xie, Y. (2015). Half-metallicity in single-layered manganese dioxide nanosheets by defect engineering. *Angewandte Chemie*, *127*(4), 1211--1215.

Wang, Y., Wang, S.-S., Lu, Y., Jiang, J., & Yang, S. (2016). Strain-induced isostructural and magnetic phase transitions in monolayer MoN2. *Nano Letters*, *16*(7), 4576-4582.

Zhuang, H., Xie, Y., Kent, P., & Ganesh, P. (2015). Computational discovery of ferromagnetic semiconducting single-layer CrSnTe3. *Physical Review B*, *92*(3), 035407.